Formation and Patterning of Self-Assembled Monolayers Derived from Long-Chain Organosilicon Amphiphiles and Their Use as Templates in Materials Microfabrication

Krista R. Finnie,[†] Rick Haasch, and Ralph G. Nuzzo*,[†,‡]

Department of Materials Science & Engineering, School of Chemical Sciences, and The Frederick Seitz Materials Research Laboratory, University of Illinois at Urbana-Champaign, Urbana, Illinois 61801

Received February 18, 2000. In Final Form: May 22, 2000

Thin films of docosyltrichlorosilane (DTS) were deposited by contact printing on the native oxide surface of a Si(100) single-crystal substrate. The nature of these thin-film layers, as characterized via ellipsometry, scanning electron microscopy, atomic force microscopy, X-ray photoelectron spectroscopy, and reflection−absorption infrared spectroscopy, show both similarities to and differences from the extensively studied monolayers derived from octadecyltrichlorosilane (OTS). The structure of these films was found to be close packed and highly oriented for all mass coverages investigated. Taken together, the data indicate that the DTS films grow via the nucleation, expansion, and eventual coalescence of islands on the substrate. The patterning abilities of DTS were also investigated by scanning electron and atomic force microscopy. These studies showed little spreading of the DTS in films patterned by microcontact printing either by edge diffusion or by island formation in the nonprinted regions. These properties, which constitute a significant improvement over previously studied alkyltrichlorosilanes, led to a more accurate transfer of the printed image. The ability of the film to serve as a wet chemical etch resist was studied and found to offer marked improvements over OTS films.

Introduction

Current methods of semiconductor device fabrication are based on complex procedures, many of which involve the sequential application of photolithography and etching processes to create patterns in materials.[1−7] These processes are extremely sophisticated and well suited to the current and projected near-term demands of device design rules.[2−5,7] Limitations do exist with these patterning methods, however, both technical and financial in nature. A consideration of these factors is useful here. First, patterning processes based on photolithography and etching are both extremely expensive and generally available only for the narrow range of materials commonly encountered in semiconductor microfabrication lines.[2,4,5,7−9] Second, due to the constraints posed by the nature and wavelength of the light projection process, photolithography will be hard to extend in a cost-effective way to nanoscale design rules[2,7,9] or integration schemes that are more than two-dimensional (the processing is typically done on interconnected planar levels which are sequentially built up).[2,3,7] Additionally, photolithography as a projection-based method of fine-scale patterning has significant limitations regarding its exposable area size which in turn significantly limits its ability to pattern very large substrates with either acceptable yields or costs.[10,11] The etching processes used in conjunction with photolithography provide another significant limitation, since not all materials are easily etched.[3,5,6,12,13] This latter fact frequently constrains the metals and ceramics that can be used in a device design. These issues have stimulated an intensive search for new, cost-effective patterning processes that overcome these limitations.[14−26] One solution attracting significant attention in current

* To whom correspondence may be addressed. E-mail: r-nuzzo@uiuc.edu. Phone: 217-244-0809. Fax: 217-244-2278.

[†] School of Chemical Sciences.

[‡] Department of Materials Science & Engineering.

(1) Mustrangels, C. H.; Tang, W. C. In *Semiconductor Sensors*; Sze, S. M., Ed.; John Wiley & Sons: New York, 1994; pp 20−30.

(2) Streetman, B. G. *Solid State Electronic Devices*; Prentice Hall: Englewood Cliffs, NJ, 1995.

(3) Mogab, C. J. In *VLSI Technology*; Sze, S., Ed.; McGraw-Hill: New York, 1983; p 303.

(4) Jones, R. E.; Desu, S. B. *MRS Bull.* **1996**, *21*, 55−58.

(5) Taylor, M. *Semicond. Int.* **1996**, 162.

(6) Singer, P. *Semicond. Int.* **1995**, 65−68.

(7) McGillis In *VLSI Technology*; Sze, S. M., Ed.; McGraw-Hill: New York, 1983; pp 267−298.

(8) Steigerwald, J. M.; Zirpoli, R.; Murarka, S. P.; Price, D.; Gutmann, R. J. *J. Electrochem Soc.* **1994**, *141*, 2842−2848.

(9) Moore, G. *Electrochem. Soc. Interface* **1997**, Spring, 18.

(10) Larson, R. G.; Rehg, T. J. In *Liquid Film Coating*; Kistler, S. F., Schweitzer, P. M., Eds.; Chapman and Hall: London, 1997; p 709.

(11) Jackman, R. J.; Wilbur, J. L.; Whitesides, G. M. *Science* **1995**, *269*, 664−666.

(12) Jeon, N. L.; Lin, W. B.; Erhardt, M. K.; Girolami, G. S.; Nuzzo, R. G. *Langmuir* **1997**, *13*, 3833−3838.

(13) Erhardt, M. K.; Nuzzo, R. G. *Langmuir* **1999**, *15*, 2188−2193.

(14) Jeon, N. L.; Hu, J. M.; Whitesides, G. M.; Erhardt, M. K.; Nuzzo, R. G. *Adv. Mater.* **1998**, *10*, 1466−1469.

(15) Xia, Y.; Whitesides, G. M. *Angew. Chem., Int. Ed. Engl.* **1998**, *37*, 550−575.

(16) Wilbur, J. L.; Kim, E.; Xia, Y.; Whitesides, G. M. *Adv. Mater.* **1995**, *7*, 649−652.

(17) Kim, E.; Kumar, A.; Whitesides, G. M. *J. Electrochem. Soc.* **1995**, *142*, 628−633.

(18) Hidber, P. C.; Helbig, W.; Kim, E.; Whitesides, G. *Langmuir* **1996**, *12*, 1375−1380.

(19) Larsen, N. B.; Biebuyck, H.; Delamarche, E.; Michel, B. *J. Am. Chem. Soc.* **1997**, *119*, 3017−3026.

(20) Kumar, A.; Biebuyck, H. A.; Abbott, N. L.; Whitesides, G. M. *J. Am. Che. Soc.* **1992**, *114*, 9188−9189.

(21) Abbott, N. L.; Kumar, A.; Whitesides, G. M. *Chem. Mater.* **1994**, *6*, 596−602.

(22) Jeon, N. L.; Clem, P. G.; Payne, D. A.; Nuzzo, R. G. *Langmuir* **1996**, *12*, 5350−5355.

(23) Jeon, N. L.; Clem, P.; Jung, D. Y.; Lin, W. B.; Girolami, G. S.; Payne, D. A.; Nuzzo, R. G. *Adv. Mater.* **1997**, *9*, 891−895.

(24) Jeon, N. L.; Finnie, K.; Branshaw, K.; Nuzzo, R. G. *Langmuir* **1997**, *13*, 3382−3391.

(25) Jeon, N. L.; Clem, P. G.; Nuzzo, R. G.; Payne, D. A. *J. Mater. Res.* **1995**, *10*, 2996−2999.

(26) Jeon, N. L.; Nuzzo, R. G.; Xia, Y.; Mrksich, M.; Whitesides, G. M. *Langmuir* **1995**, *11*, 3024−3026.

10.1021/la000245p CCC: $19.00
Published on Web 07/20/2000

research is the related technologies of soft-lithographic patterning.[12−18,24,27] This paper is primarily concerned with the formation and subsequent use of thin-film templates (resists), ones patterned via microcontact printing (μ-CP).[12,15−18,22−28] This method is well developed as a means of patterning diverse material types and is especially well suited to the generation of patterned structures in self-assembled monolayers (SAMs).

SAMs themselves have been studied for some time in part because of their potential applications in materials chemistry.[16−18,21,24,29−37] The most widely studied and best understood SAM systems are those formed by alkanethiols on gold[15−17,19−21,27,28,35,37−41] and functional organosilanes on silicon and other oxide-bearing substrates.[15,24,29,30,32,35,39,42] Alkanethiol SAMs on gold[16,20,21,27,28,41] and silver[28] have been investigated and found to function as exceedingly effective wet chemical etch resists. The SAMs formed by organosilanes on Si, however, have a more limited utility in patterning. They are very effective resists for lift-off based patterning,[22,23] but are not at all suitable for wet[42] or ion-beam-mediated etching processes.[43,44]

The structure of alkyltrichlorosilane SAMs on silicon has also been studied extensively.[19,24,32,39,42,45,46] In this paper, we present the results of a study which explored methods to improve the functioning of organotrichlorosilanes on silicon as direct etch resists. Previous investigations have shown that patterned SAMs of octadecyltrichlorosilane (OTS), when printed on a silicon substrate, can be used as a resist in several processes, including directed deposition of metal thin films by chemical vapor deposition (CVD)[12,22,24,26] and the patterned sol−gel deposition of ceramic thin films.[23,25] Combined additive and soft-lithographic patterning techniques also have provided new pathways for fabricating microelectronic devices, including capacitor arrays,[23] field effect transistors,[14] and platinum silicide Schottky diodes.[23]

These studies revealed several problems with the use of OTS thin films as resists. Of most concern, an examination of patterned OTS SAMs by scanning electron (SEM) and atomic force (AFM) microscopies revealed that the contact between the stamp and the surface led to a time-dependent spreading of the pattern, which in turn reduced the edge resolution and dimensional fidelity of the pattern transferred.[24] It was also found that OTS islands migrate into the unpatterned regions, thus further reducing the fidelity of the pattern transfer. These defects reduce the resolution achievable in patterned OTS films, especially for feature sizes approaching the submicrometer scale. The mechanism of this migration has yet to be determined, but we hypothesized that the islands form either by vapor-phase transport or lateral migration on the surface.[24] One intuitive approach to eliminating this deficiency is to use an alkyltrichlorosilane "ink" that has a lower vapor pressure and/or lower lateral mobility than OTS. This may be accomplished by selecting an alkyltrichlorosilane with a longer hydrocarbon chain.

For this study, an alkyltrichlorosilane with a normal hydrocarbon chain length of 22 carbons, docosyltrichlorosilane (DTS), was chosen. As we will show, extending the hydrocarbon chain length from 18 (for OTS) to 22 carbon atoms (for DTS), dramatically impacts the transfer fidelity and etch resistance of the μ-CP patterned SAMs. The structure of these contact-printed DTS films on silicon was characterized by ellipsometry, X-ray photoelectron spectroscopy (XPS), and reflection−adsorption infrared spectroscopy (RAIRS). The patterns formed by the DTS ink were analyzed by SEM and AFM, and their suitability as a wet chemical etch resist was tested using a 4 M KOH etching bath.

Experimental Section

Materials and Film Formation. The substrates used in these experiments were Si(100) wafers (test grade, p-type, obtained from Silicon Sense, Nashua, NH). The substrates were cut into ~4 cm^2 pieces for further modification. The substrates were cleaned by repeated rinsing with deionized water, acetone, and isopropyl alcohol and dried under a nitrogen stream. The substrates were exposed, in a home-built UV/ozone chamber (low-pressure mercury lamp, $\lambda = 185$ and 254 nm), for 15 min prior to modification to remove hydrocarbon impurities and produce a hydrophilic surface. The DTS films were made by spin coating a patterned (or unpatterned) poly(dimethylsiloxane) (PDMS) stamp using a photoresist spinner (Headway Research, Garland, TX) with a freshly prepared 10 mM solution of docosyltrichlorosilane (Gelest, Tullytown, PA) dissolved in hexane (Aldrich, Milwaukee, WI) at 3000 rpm for 30 s. The stamp was then dried under a nitrogen stream for 30 s, and then brought into contact with the substrate for a predetermined length of time (typically a contact time of ≥30 s was used). Reference DTS films were formed by immersion of a freshly cleaned substrate for 30 min into a solution of docosyltrichlorosilane (Gelest, Tullytown, PA) dissolved in toluene (distilled under N_2 from calcium hydride). Contact-printed DTS films were formed by first spin coating a PDMS stamp four times, drying the stamp under a nitrogen stream for 30 s, and then bringing the stamp into contact with the substrate for 1−5 min. During the printing process, the substrate temperature (and thereby the stamp surface equilibrated against it) was held at various temperatures, ranging from 25 to 45 °C using a programmable thermal block heater (Fisher Scientific, Pittsburgh, PA). The humidity levels present during the reaction were also varied, from low relative humidities (near 30%) to high relative humidities (near 60%), using either variations in the laboratory ambient or a controlled humidity enclosure (the latter was constructed by mounting a Duracraft humidifier in a decommissioned, sealable fume hood). After the films were formed, the samples were either used as printed or annealed for 1 h at 75 °C. The PDMS stamps used in these experiments were fabricated according to previously reported

(27) Kumar, A.; Biebuyck, H. A.; Whitesides, G. M. *Langmuir* **1994**, *10*, 1498−1511.
(28) Xia, Y.; Zhao, X.; Whitesides, G. M. *Microelectron. Eng.* **1996**, *32*, 255−268.
(29) Allara, D. L.; Nuzzo, R. G. *Langmuir* **1985**, *1*, 45−52.
(30) Allara, D. L.; Nuzzo, R. G. *Langmuir* **1985**, *1*, 52−66.
(31) Boerio, F. J.; Boerio, J. P.; Bozian, R. C. *Appl. Surf. Sci.* **1988**, *31*, 42−58.
(32) Allara, D. L.; Parikh, A. N.; Rondelez, F. *Langmuir* **1995**, *11*, 2357−2360.
(33) Dubois, L. H.; Nuzzo, R. G. *Annu. Rev. Phys. Chem.* **1992**, *43*, 437−463.
(34) Whitesides, G. M.; Gorman, C. B. In *Handbook of Surface Imaging and Visualization*; Hubbard, A. T., Ed.; CRC Press: Boca Raton, FL, 1995; pp 713−733.
(35) Ulman, A. *An Introduction to Ultrathin Organic Films from Langmuir−Blodgett to Self-Assembly*; Academic: San Diego, CA, 1991.
(36) Calvert, J. M. In *Organic Thin Films and Surfaces*: *Directions for the Nineties*; Ulman, A., Ed.; Academic: San Diego, CA, 1993; Vol. 20, pp 109−141.
(37) Nuzzo, R. G.; Allara, D. L. *J. Am. Chem. Soc.* **1983**, *105*, 4481−4483.
(38) Laibinis, P. E.; Bain, C. D.; Nuzzo, R. G.; Whitesides, G. M. *J. Phys. Chem.* **1995**, *99*, 7663−7676.
(39) Hoffmann, H.; Mayer, U.; Krischanitz, A. *Langmuir* **1995**, *11*, 1304−1312.
(40) Bain, C. D.; Whitesides, G. M. *Angew. Chem., Int. Ed. Engl.* **1989**, *28*, 506−512.
(41) Kumar, A.; Whitesides, G. M. *Appl. Phys. Lett.* **1993**, *63*, 2002−2004.
(42) Wasserman, S. R.; Tao, Y.; Whitesides, G. M. *Langmuir* **1989**, *5*, 1074−1087.
(43) Lercel, M. J.; Craighead, H. G.; Parikh, A. N.; Seshadri, K.; Allara, D. L. *J. Vac. Sci. Technol., A* **1996**, *14*, 1844−1849.
(44) Seshadri, K.; Froyd, K.; Parikh, A. N.; Allara, D. L.; Lercel, M. J.; Craighead, H. G. *J. Phys. Chem.* **1996**, *100*, 15900−15909.
(45) Hoffmann, H.; Mayer, U.; Brunner, H.; Krischanitz, A. *Vib. Spectrosc.* **1995**, *8*, 151−157.
(46) Parikh, A. N.; Allara, D. L.; Ben Azouz, I.; Rondelez, F. *J. Phys. Chem.* **1994**, *98*, 7577−7590.

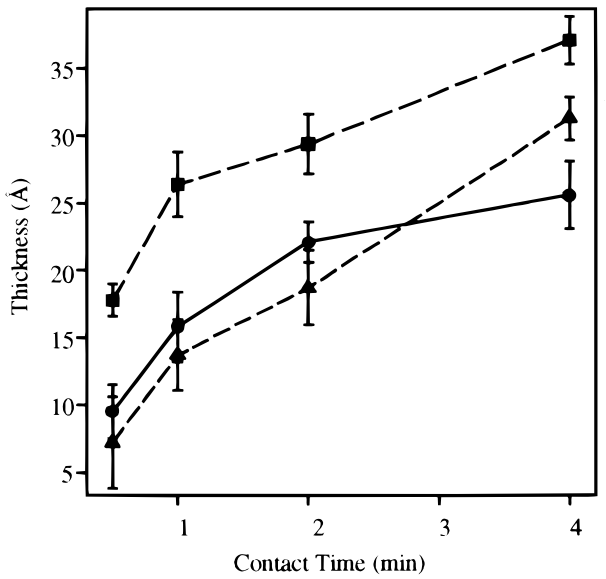

Figure 1. Effect of printing contact time and temperature on film thickness for DTS film deposited by contact for room temperature (▲), at 30 °C (●), and at 40 °C (■).

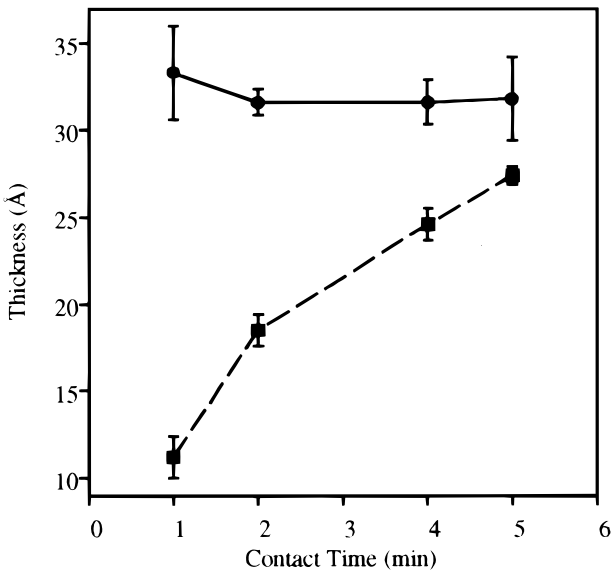

Figure 2. Effect of humidity on mass transfer during the printing process for high (●) and low (■) relative humidity. High humidity accelerates the film formation process, forming a monolayer equivalent after 1 min of contact time, as opposed to 5 min for low humidity conditions.

methods and rinsed with isopropyl alcohol prior to each use.[20,27,41] Samples were etched for 5−15 min in a 4 M KOH/15% isopropyl alcohol solution held at 35 °C.

Ellipsometry. Ellipsometric measurements were made with a Gaertner Scientific (Chicago, IL) model L116C ellipsometer equipped with a He−Ne laser set at an incidence angle of 70°. Measurements were taken at 8−10 points randomly selected across the surface and averaged. A two-layer transparent film model was used for the thickness calculations based on pseudosubstrate constants measured on the clean substrate. The refractive index of the organic film was fixed at 1.5. The contact-printed SAMs used for these measurements were formed using a planar (unpatterned) PDMS stamp.

X-ray Photoelectron Spectroscopy (XPS). XPS data on planar (unpatterned) DTS films were collected using a Perkin-Elmer/Phi XPS 5400 spectrometer using Mg Kα radiation (15 kV, 400 W). The data were collected for a variety of sample tilt angles (60°, 30°, and 15°) and for differing stamp contact times. Photoelectrons were analyzed using a hemispherical analyzer at a constant pass energy of 178.95 eV.

Reflection−Absorption Infrared Spectroscopy (RAIRS). An external reflection−absorption infrared spectroscopy optical bench was used in conjunction with a conventional Fourier transform spectrometer (Bio-Rad FTS-60). The light in the external beam was incident on the sample at a grazing angle of ∼84°. The reflection optics were optimized at ∼×a6/12, and the incident radiation was p-polarized. The signal was detected by a liquid nitrogen cooled narrow band MCT detector. The spectra were recorded at a resolution of 4 cm^{-1} using 4096 scans and a 20 kHz modulation. Freshly cleaned silicon substrates without the DTS films were used as a reference, and the data are reported in the absorbance format ($-\log R/R_0$). The samples were planar (unpatterned) DTS films with different stamp contact times.

Scanning Electron Microscopy (SEM). SEM micrographs of patterned DTS films were acquired using a Hitachi S-800 microscope. The accelerating voltage was set to 20 kV and the sample tilt angle at 0°. Images were acquired at several magnifications as indicated in the micrographs.

Atomic Force Microscopy (AFM). A Digital Instruments Dimension-3000 scanning probe microscope was used to acquire AFM images of patterned DTS films. A standard Si_3N_4 tip was used, and the images were acquired in the contact mode with a scan rate of 1 Hz and contact forces reduced to the minimum necessary to maintain feedback.

Results

Mass Coverage of DTS−SAMs Prepared by Contact Printing As Deduced by Ellipsometry. Figure 1 shows the thickness of contact-printed DTS films on Si(100) as a function of the contact time and substrate temperature used. The data suggest that a thickness equivalent to that of a full monolayer of DTS (∼29 Å) can be achieved on a sample held at ambient temperature with a stamp contact time in the range of 4 min. Increasing the substrate temperature generally leads to an increase in the film thickness at comparable contact times although, as noted in the figure, the system shows a degree of sample to sample variability (we believe that changes in the ambient humidity are responsible for most of this sensitivity). In general terms for the stamps and inking procedures used here, higher temperatures and longer contact times yield higher mass coverage films. The assembly times needed to reach a limiting value of the mass coverage close to that of a monolayer are always longer than that found for OTS, however. These effects are most likely attributable to the higher melting point of DTS compared to OTS (25−40 °C for DTS, while OTS is a liquid at room temperature).

The contact time required to achieve a thickness equivalent to a full monolayer varies sensitively with the relative humidity, as is illustrated by the data presented in Figure 2. Higher relative humidity reduces the contact time necessary to achieve a formal mass coverage of one monolayer. For example, a thickness corresponding to a full monolayer was achieved after 1 min of contact at 45 °C in high relative humidity, as opposed to 5 min of contact being required to reach a similar mass coverage at 45 °C in low relative humidity. Additionally, it is interesting to note that at high humidity, the film thickness remains fairly consistent at all contact times. This is in direct contrast with the data obtained for contact-printed OTS films, whose film thicknesses continued to increase, reaching (and eventually exceeding) multilayer thicknesses. As a result of these experiments, the controlled humidity stamping environment described above was created, to ensure high ambient humidity levels during stamp preparation and printing.

X-ray Photoelectron Spectroscopy of DTS Films. Figure 3 shows representative spectra measured on DTS films printed (under low humidity) with varying contact

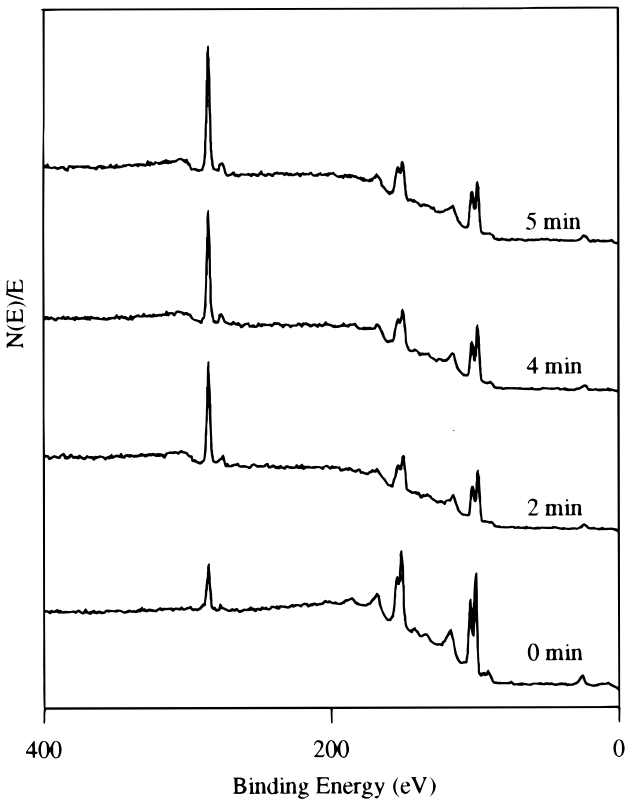

Figure 3. Spectra obtained using a 45° takeoff angle of DTS films on silicon printed at 2, 4, and 5 min contact times.

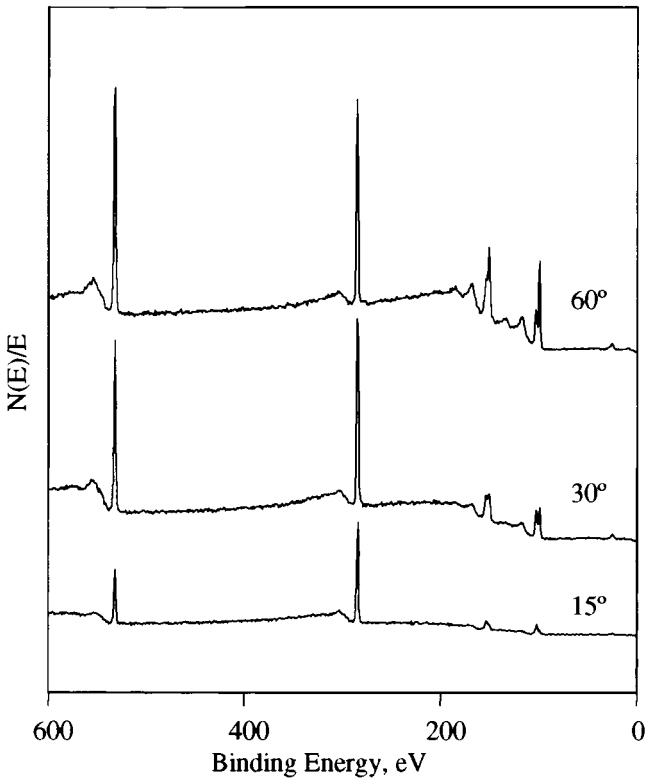

Figure 4. Spectra obtained at different takeoff angles for a high coverage printed (5 min) DTS SAM.

times. These spectra show that the intensities of the core level signals corresponding to the substrate [Si(2s) (∼155 eV), and Si(2p) (∼103 eV)] decrease as expected with increasing the stamp contact time. These trends mirror the increasing mass-coverage of the OTS chains revealed by the ellipsometry data. As expected for an organized DTS SAM, the carbon peak intensity [C(1s) (284.5 eV)] shows a corresponding increase. These results thus support the suggestion, even on a qualitative basis, that the film coverage increases with the stamp contact time.

The trends evidenced in the data shown in Figure 3 can be analyzed more quantitatively via the takeoff angle dependence of the core level intensities. Such an examination was performed on a sample bearing a mass coverage of DTS near one monolayer (as determined by ellipsometry and as obtained for a stamp contact time of 5 min). These data are shown in Figure 4. At more surface-sensitive takeoff angles (15°) the substrate Si(2p) and Si(2s) peak intensities are weak in comparison to the C(1s) core level peak. As the takeoff angle is increased to more bulk sensitive values, the relative scaling of these core level intensities changes markedly. The Si(2p) and (2s) core level intensities increase significantly. The spectra further show the complex nature of the substrate, namely, that the Si(100) substrate bears a thin (∼15 Å) native oxide. Thus at the highest takeoff angles, the elemental Si of the bulk substrates contributes most significantly but is rapidly attenuated at shallower takeoff angles by both the native oxide layer and the hydrocarbon chains of the DTS SAM. The thickness of the DTS SAM in principle can be calculated from its attenuation of the substrate signal. This calculation, if based on the angular dependences of the C(1s) and a Si derived core level, is a reasonably complex one for the multilayer Si(100)·SiO_2·DTS structure and requires a number of simplifying assumptions that offer little advantage over those used to model the ellipsometry data. The most significant of these simplifying assumptions neglects elastic scattering due to photoelectron diffraction from the Si(100) substrate.[47] (Elastic electron scattering effects become significant at takeoff angles less than 45°.)

On the basis of a two-layer model described elsewhere[48] (which accounts for only inelastic scattering) the following equation may be derived

$$\frac{d}{\lambda} = \ln\left(\frac{c_a}{c_b} + 1\right) \sin\theta$$

where c_a is the overlayer atomic concentration, c_b is the substrate atomic concentration, θ is the takeoff angle relative to the surface, and λ is the inelastic electron mean free path.

Using the ratios of the C-to-O and the C-to-Si core-level intensities data at $\theta = 60°$, and assuming a uniform value for λ, we calculate that the chain thickness giving this effect is ∼30 Å. These results thus serve to support the interpretations of the trends seen in the ellipsometry data and further serve to confirm that the stamp contact time required to deposit an DTS film of one monolayer mass coverage leads to the formation of a coherent monolayer (rather than a more granular) structure.

DTS Film Structure As Deduced by RAIRS. Figure 5 shows the RAIR spectra in the C−H stretching region for DTS films on silicon both formed by contact printing (Figure 5A) and assembled by immersion in an adsorbate-containing solution (10 mM DTS in toluene, Figure 5B). For all of the contact times, the printed films show similar dichroism (albeit with different absolute intensities) in the two positive intensity peaks seen at 2850 and 2917

(47) Baschenko, O.; Nefedov, J. *J. Electron Spectrosc.* **1980**, *17*, 153.
(48) Briggs, D.; Seah, M. P. *Practical Surface Analysis*, 2nd ed.; Briggs, D., Seah, M. P., Eds.; John Wiley & Sons: New York, 1996; Vol. 1.

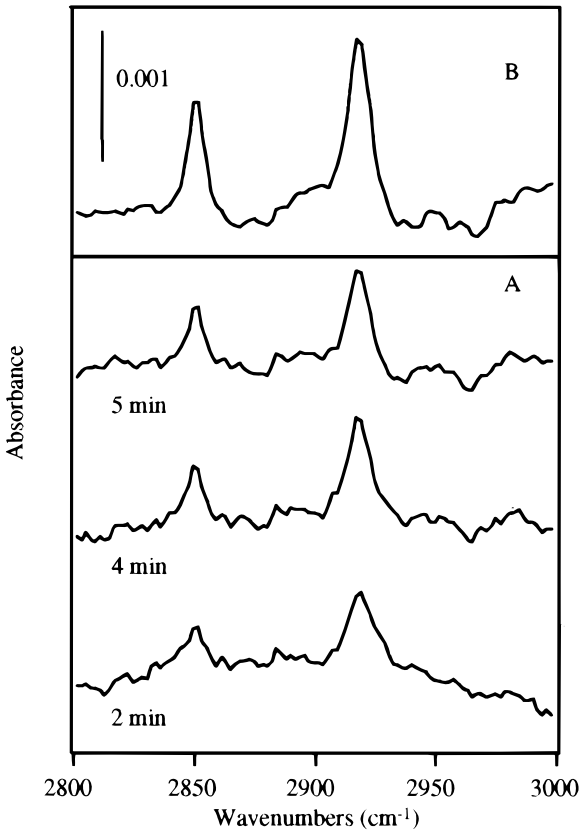

Figure 5. (A) RAIR spectra of DTS printed at room temperature for varying contact times; compared to (B) RAIR spectra of DTS film formed by immersion for 30 min, presented on the same intensity scale.

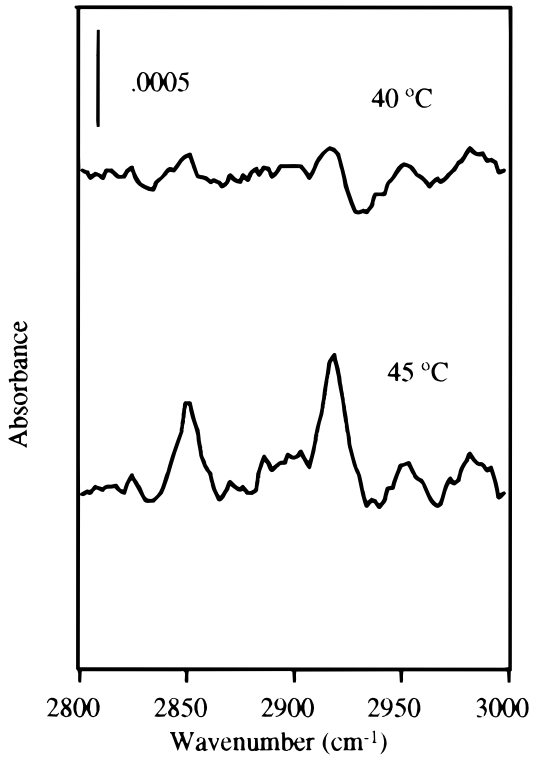

Figure 6. RAIR spectra of DTS films printed at elevated temperatures. A contact time of 5 min was employed.

cm^{-1} and weaker negative intensity feature appearing at 2967 cm^{-1}. The line widths narrow somewhat at longer contact times. A similar pattern of bands is seen in the spectrum obtained for the sample prepared by immersion, although with some minor differences in the intensity being noted. The positive intensity bands are assigned to the symmetric [$\nu_s(CH_2)$, 2850 cm^{-1}] and the antisymmetric [$\nu_{as}(CH_2)$, 2917 cm^{-1}] methylene stretches, respectively, while the weak negative intensity band is most likely due to the antisymmetric in-plane methyl-stretching mode [ν_{as}-$(CH_3)_{ip}$, 2967 cm^{-1}].[31,39,45,49−61] The complexity of these spectra, being comprised of both positive and negative intensity features, arises as a direct result of the optical properties of both DTS and the silicon substrate used in this experiment as well as the organizational properties of the SAM.[39,45,49−51,57,58,61,62] We defer further discussion of this point until later.

The ellipsometry data presented above reveal that the substrate temperature sensitively impacts the printing of DTS thin films. We examined the character of this influence via vibrational spectroscopy. Figure 6 shows RAIR spectra measured in the C−H stretching region for DTS films prepared by contact printing on substrates held at elevated temperatures (40 and 45 °C, respectively). A common contact time of 5 min was used in both cases. It is interesting to note that the spectra show marked differences in both the intensities and the line shapes of the component bands. Although the nominal peak positions of the identifiable bands are similar to those seen in the room-temperature studies, the changing line shapes suggest differences exist in the organizational structure of the chains. At 45 °C, the films transferred after a 5-min contact time appear to exhibit a larger mass coverage and improved film structure vis-à-vis the presence of conformational defects (see below). These results are consistent with the temperature-related trends seen in the ellipsometry data.

Contact Printing of Patterned DTS Films. Figure 7 shows AFM images of patterned DTS films printed in a high-relative-humidity ambient on Si(100)·SiO_2 substrates held at 45 °C for a variety of stamp contact times. The master used to construct this patterned stamp was based on a mask for an interdigitated array electrode with 15 μm lines and spaces. These images clearly show that the printed films, regardless of contact time, retain the dimensions of the master pattern, with no noticeable line spreading (as was found for OTS-derived SAMs).[24] Additionally, little or no island budding near the line edge is apparent for the shorter contact times; at the longer contact times which give higher mass coverage SAMs, some such island formation is visible. A closer examination of the films formed with longer contact times shows the extent of this island formation and migration (Figure 8). For a contact time of 4 min in a 25 μm^2 field of view,

(49) Allara, D. L. *Crit. Rev. Surf. Chem.* **1993**, *2*, 91−110.
(50) Parikh, A. N.; Allara, D. L. *J. Chem. Phys.* **1992**, *96*, 927−945.
(51) Hoffmann, H.; Mayer, U.; Brunner, H.; Krischanitz, A. *J. Mol. Struct.* **1995**, *349*, 305−308.
(52) Greenler, R. G. *J. Vac. Sci. Technol.* **1975**, *12*, 1410−1417.
(53) Harrick, N. J. In *Characterization of Metal and Polymer Surfaces—Polymer Surfaces*; Lee, L. H., Ed.; Academic Press: New York, 1977; Vol. 2, pp 152−192.
(54) Ishino, Y.; Ishida, H. *Langmuir* **1988**, *4*, 1341−1346.
(55) Jasse, B.; Koenig, J. L. *J. Macromol. Sci.—Rev. Macromol. Chem.* **1979**, *C17*, 61−135.
(56) Mielczarski, J. A.; Yoon, R. H. *J. Phys. Chem.* **1989**, *93*, 2034−2038.
(57) Mielczarski, J. A. *J. Phys. Chem.* **1993**, *97*, 2649−2663.
(58) Porter, M. D. *Anal. Chem.* **1988**, *60*, 1143A-1155A.
(59) Tompkins, H. G. *Appl. Spectrosc.* **1976**, *30*, 377−383.
(60) Chabal, Y. *J. Phys. Chem.* **1988**, *8*, 211−357.
(61) Chabal, Y. J. *Surf. Sci. Rep.* **1988**, *8*, 211−357.
(62) Yen, Y.; Wong, J. *J. Phys. Chem.* **1989**, *93*, 7208−7216.

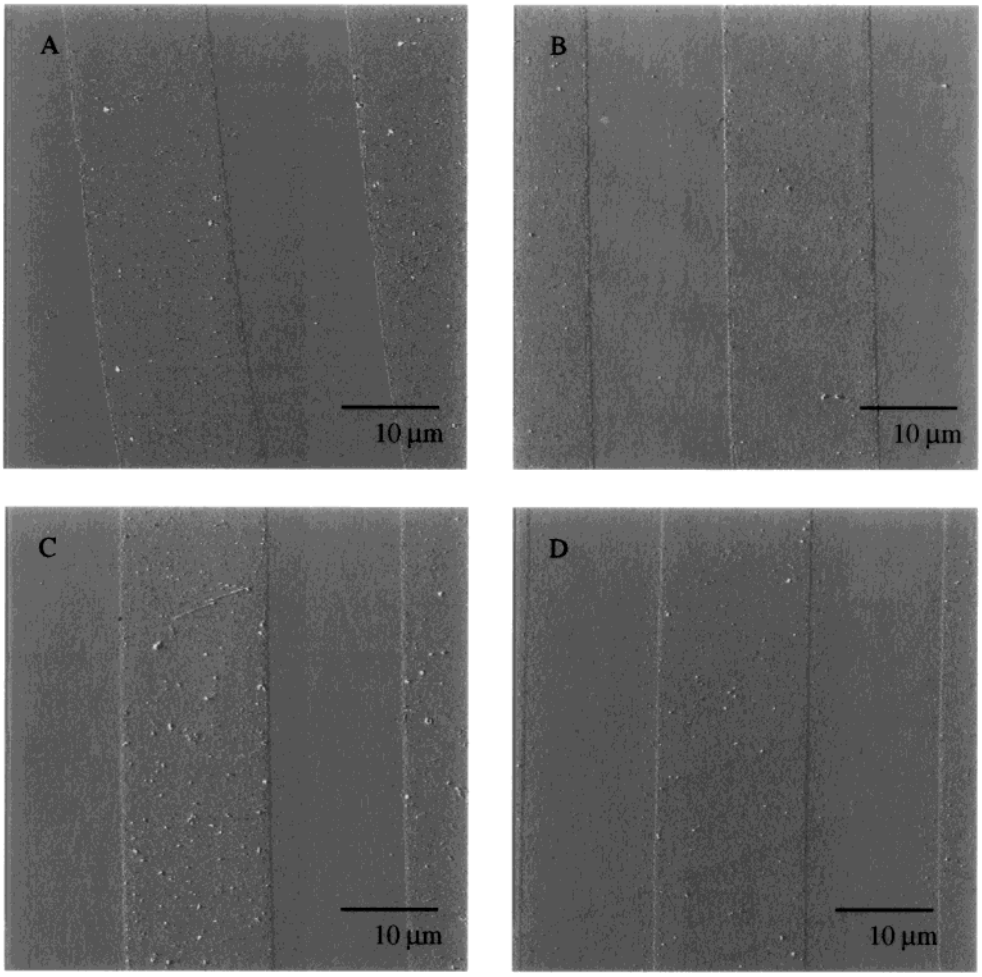

Figure 7. AFM images of DTS films printed at 45 °C with contact times of (A) 1 min, (B) 2 min, (C) 4 min, and (D) 5 min.

several small islands and a few larger islands are observed within approximately 0.25 μm of the line edge. For a 5 min contact time, the number and size of the islands increased ($\sim$3$\times$ and 2$\times$, respectively), with the shape of the larger islands suggestive of a clustering of smaller islands. The islands also appeared to have migrated further, with the majority of the islands remaining within $\sim$1 μm of the line edge. Additionally, for both contact times, the edge of the printed line shows a modest corrugation when compared to the 15 μm line width. This corrugation (and the islands) would be a more significant problem for submicrometer scale patterning, though. We see from these data that even though the problem of island migration has not yet been completely eliminated, the number of islands seen for printed DTS films is significantly lower than that for printed OTS films (we estimate for even the worst case example shown here, by at least a factor of $10-10^2$) and are forming appreciably only after much longer contact times.

Patterned DTS Films as Etch Resists. Figure 9 shows SEM images of the surface of a Si single-crystalline substrate modified by printing a patterned DTS film at room temperature, annealing the sample at 75 °C for 1 h in air, and then etching it for 10 min in a 4 M KOH solution held at 35 °C. This procedure, which etches $\sim$140 nm of Si in this time, was adopted based on screening experiments which showed that annealing the sample prior to etching improved the ability of the film to act as a resist. The pattern printed here corresponds to 15 μm lines with 15 μm spaces. OTS films lead to no viable pattern transfer under these conditions. Pattern transfer is seen for the DTS SAMs, however. Unfortunately, as is evident by the large number of defects seen in this figure, the DTS film failed to sufficiently protect the printed regions, leaving complex defect patterns etched deeply into the printed regions. This defect structure suggests that the DTS film was formed from individual clusters of DTS, ones which had not completely coalesced to form a cohesive film. We therefore experimented further to determine whether this problem might be solved by elevating the substrate temperature to 45 °C during the initial printing above the melting point of DTS.

SEM images (Figure 10) of etched samples prepared in this way (again a postprinting annealing step was used) show a dramatic improvement over the previous samples. The defects clearly evident in Figure 9 are no longer visible; instead, the printed lines appear to be virtually defect free. Upon closer examination of the etched sample by AFM (the data for which are shown in Figure 11) we did in fact confirm the presence of several types of defects in the etched sample. First, the printed regions show some etch pits where the SAM failed to sufficiently protect the underlying silicon surface. Additionally, defects in the unpatterned regions are also visible. It is interesting to note that the DTS islands visible in Figure 8 actually survive the etching process. We are intrigued by the pattern transfer seen here and are currently exploring ways to engineer the formation of latent images via the phase dynamics of a thin-film SAM template. Despite these remaining defects, these samples show a significant improvement over films printed at room temperature and suggest further room surely exists to improve the per-

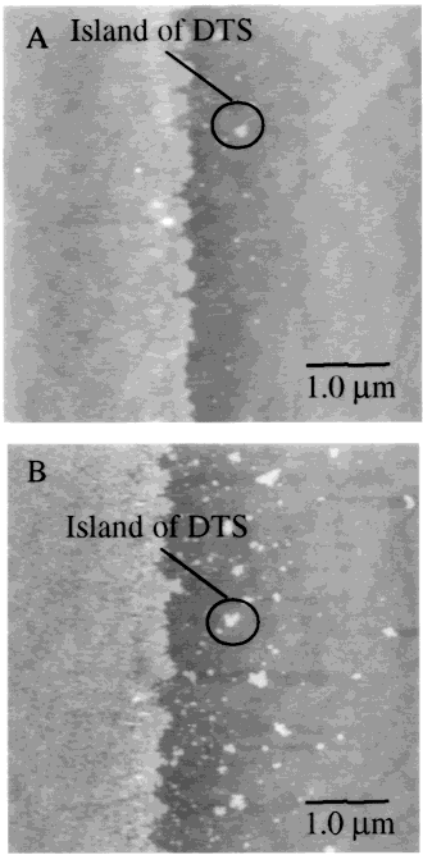

Figure 8. Expanded view of AFM images near the SAM line edge for of DTS lines printed using contact times at 45 °C of (A) 4 min and (B) 5 min.

formance of μ-CP inks for silicon substrates via rational synthetic design.

Discussion

Film Structure and Characterization. Taken together, the data obtained from ellipsometry, XPS, and RAIRS measurements provides information from which we can deduce the general structure and molecular organization of printed DTS films. As previously mentioned, the ellipsometry results indicate that the DTS film formation is both time and humidity sensitive. While OTS had also shown a time dependence, the contact time required to form a dense DTS film is considerably longer than for OTS (5 min contact time for DTS as opposed to 30 s contact time for OTS) under comparable conditions. The longer time necessary for film formation with the former can be attributed to the change in the physical properties associated with its longer chain length and perhaps lower vapor pressure as well. Together, these physical changes contribute to a marked reduction in the kinetics of film formation. Steric (i.e., chain length dependent) inhibition has been noted in the assembly of other SAM systems (e.g., thiols on Au and Ag substrates) but mostly for preparations using a solution immersion method.[29,30,33,34,37,63]

It has been shown previously that the presence of water is necessary for the formation of OTS SAMs.[32,46] This water forms as an ultrathin layer on the surface and obtains partly as a result of the humidity present in the air. This thin layer of water aides the silicon oxide layer in forming covalent and physical bonds with the film and ultimately

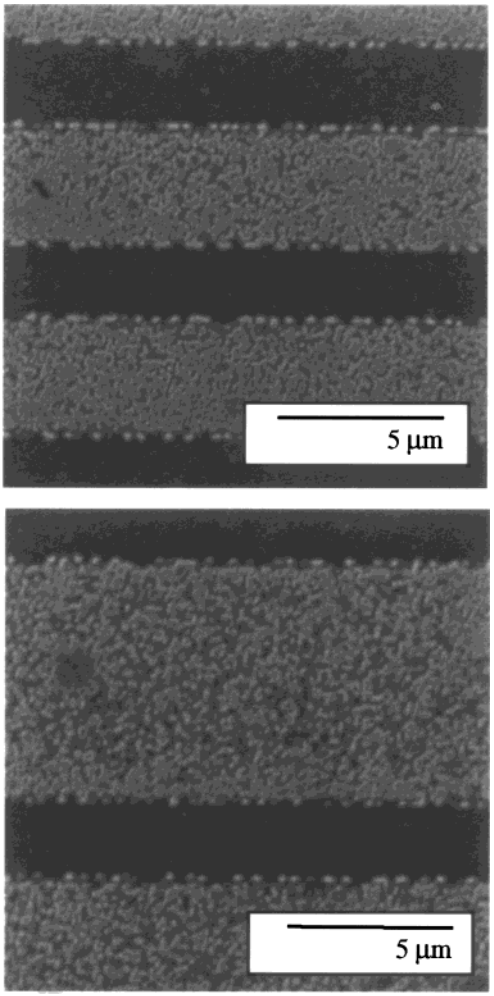

Figure 9. SEM images of a DTS film, formed by contact printing for 5 min, annealing the sample in air for 1 h at 75 °C, and then etched for 10 min in a 4 M KOH solution held at 35 °C.

leads to the hydrolysis of the alkyltrichlorosilane, a step necessary for film formation. It is therefore not altogether surprising that the DTS film formation via contact printing, as is evidenced by the ellipsometry data, is also found to be sensitive to the relative humidity of the ambient atmosphere in which the printing processes are carried out. A similar, albeit less pronounced, sensitivity was seen with OTS as well where higher moisture levels were found to aid the film formation process.[32,42,46,64] This differing sensitivity correlates with the observation that the surface reactions for DTS are appreciably slower. It is not clear where the effects of humidity on the printing process are most strongly manifested. It is possible that it may lead to reactions of the Si−Cl bonds on the stamp as well as lead to the necessary thin water films on the oxide-bearing substrate.

Be this as it may, the ellipsometry data clearly demonstrate the necessary contact times for the varied reaction conditions which yield a thickness equivalent to a close-packed monolayer of DTS chains. These same data are somewhat information poor as they provide little evidence as to the possible orientational chain ordering in the film formed. To more closely examine the organizational characteristics of the film structure, especially as it relates to the average molecular orientation, a more detailed analysis of the XPS and RAIRS data is required.

(63) Ulman, A. *Chem. Rev.* **1996**, *96*, 1533−1554.

(64) Tripp, C. P.; Hair, M. L. *Langmuir* **1992**, *8*, 1120−1126.

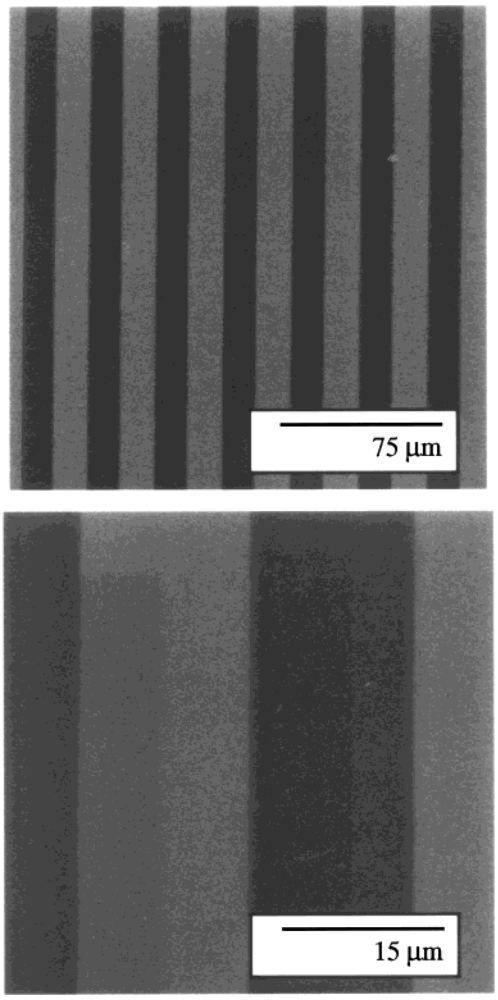

Figure 10. SEM images of a DTS film, formed by contact printing for 5 min at 45 °C, followed by annealing for 1 h at 75 °C, and then etched for 10 min in a 4 M KOH solution held at 35 °C.

The XPS data, taken for various contact times and takeoff angles, strongly confirm and extend the results obtained by ellipsometry, namely, that contact printing deposits a monolayer mass coverage as a dense 2D assembly of chains. These data further suggest strongly that the film is oriented as expected, with the silicon headgroup attached to the surface and the hydrocarbon chain pointing away from the surface toward the ambient interface (a feature more trivially established by the extreme hydrophobicity of the transferred SAM).

Further insights concerning the film structure and general molecular organization of the chains can be gleaned from the RAIRS data. It is necessary to consider the selection rules which operate here first. For metal substrates, the surface selection rules are fairly simple in that an IR beam incident at grazing angles can only excite vibrational modes with transition dipole moments projecting along the perpendicular direction to the surface.[49,52,57,60,61,65−69] Transition moments projecting

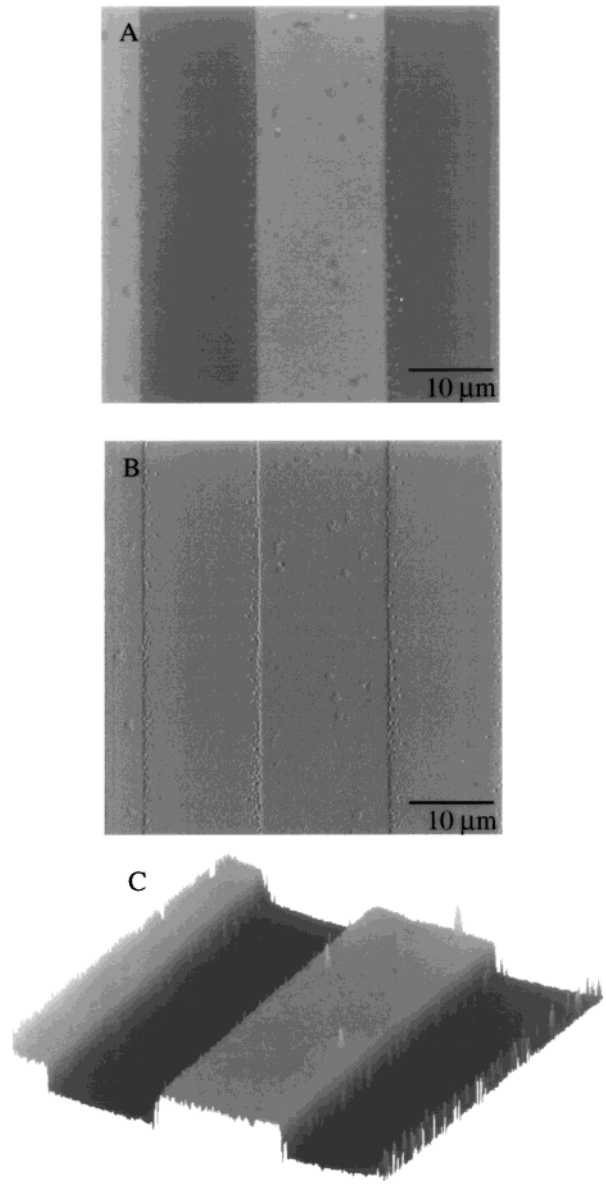

Figure 11. AFM images of a DTS film, formed by contact printing for 5 min at 45 °C, followed by annealing for 1 h at 75 °C, then etched for 10 min in a 4 M KOH solution held at 35 °C. Image (A) is height mode, (B) is deflection mode, and (C) is a surface plot.

along the parallel direction to the surface cannot be excited and, thus, are not detected. Such spectra are dominated by contributions arising from the imaginary part (i.e., the absorption index) of the complex optical function (and for that reason the line shapes in RAIRS data generally approximate those expected for a normal absorption spectrum).[45,49,50,58,61,65−69] On a less conductive substrate, such as the silicon used here, sizable electric fields exist for both perpendicular and parallel excitation polarizations, thus allowing the detection of either projection of a suitable transition dipole moment by a p- or s-polarized beam.[39,45,49−51,61,66−69] In these latter experiments, given the quantitative aspects of the optics involved, both the real and imaginary components of the complex optical functions can contribute significantly to the measured band intensities.[49,50,61,65−69] One therefore expects to see more prominent contributions (or at least potentially so) being made to the line shapes by dispersion.[49,50,65−69] The spectra shown in Figures 5 and 6, which were measured at a grazing angle of incidence with a p-polarized beam,

(65) Porter, M. D.; Bright, T. B.; Allara, D. L.; Kuwana, T. *Anal. Chem.* **1986**, *58*, 2461−2465.
(66) Chabal, Y. J. In *Semiconductor Interfaces*: *Formation and Properties*; Lelay, G. a. D., J., Ed.; Springer: Berlin, 1987; Vol. 22, p 301.
(67) Chiaradia, P. In *Semiconductor Interfaces*: *Formation and Properties*; Lelay, G. a. D., J., Ed.; Springer: Berlin, 1987; p 290.
(68) Harrick, N. J. In *Internal Reflection Spectroscopy*; Wiley: New York, 1979; pp 42−44.
(69) Olmstead, M. A. *Surf. Sci.* **1986**, *6*, 159.

do in fact show a complex overlay of positive and negative intensity features. Contributions from the imaginary part of the complex function (i.e., the "absorption index") always lead to a loss of energy from the reflected beam. The negative intensity features then (presuming the spectra have been properly compared to a clean reference sample) must arise from the contributions made by dispersion.[70] The dichroism present in these spectra suggests that the average orientation of the adsorbed chains is highly anisotropic.[39,45,49−51,61] The most significant feature of note is that the bands present in a spectrum measured with p-polarized light are in fact weak. More specifically, the weak positive intensities and narrow line widths observed for the [$\nu_s(CH_2)$] and the [$\nu_{as}(CH_2)$] strongly suggest that the transition dipole moments for these modes project strongly on directions parallel to the plane of the surface (these modes would be more sensitively probed by an s polarized beam). The weak negative intensity seen in the [$\nu_{as}(CH_3)_{ip}$] mode is indicative of a relatively stronger contribution being made to the line shapes of this feature by optical dispersion (as is consistent with quantitative analyses of related systems presented elsewhere)[39,45,49−51,61,66−68] which in turn varies sensitively with the orientation of the methyl groups. These optical anisotropies are consistent with an extended, largely all-trans configuration for the hydrocarbon chain, one aligned nearly normal to the surface, and follows closely the patterns described in the literature of similar organized assemblies.[39,45,51]

It is interesting to note that regardless of the reaction conditions (contact time and temperature, etc.), the methylene and the methyl peak positions seen in the RAIR spectra fall at nearly the same positions. The line shapes also show little variance. The largest differences seen in the RAIR spectra concern the band intensities, with films printed at higher temperatures having a slightly larger optical density. These latter differences suggest that small variations in the average tilt angles of the chains result from such variations in the printing conditions. Even so, the modest nature of these changes suggests that, in all cases, the films deposited by the contact printing process exhibit similar organized structures, despite having vastly different mass coverages. It thus appears that at shorter contact times and lower temperatures, deposition occurs by an island growth mechanism, where lateral interactions maintain a low density of conformational defects in the chains bound in each island even when the mass coverage remains relatively low. As the coverage increases, the islands coalesce to form a more coherent film. Across these limits of coverage, though (whether in an island or a full coverage SAM), the chains orient very closely along the surface normal direction. This hypothesis is further supported by the results of the etching studies, which are discussed below.

Patterned DTS Films. The AFM and SEM data reveal that DTS can be effectively patterned at the micrometer scale by μ-CP. The DTS-based ink gives good fidelity in the transferred pattern even at long contact times. This improved resistance to line spreading and island aggregation in the noncontact areas of a fine line pattern reflects a significant improvement of the ink's performance over those (such as OTS) previously described in the literature.[24] The print contact times for DTS are longer, however, and its sensitivity to the ambient humidity level makes it a somewhat difficult process to optimize. The edge roughness on the printed patterns is one structural aspect that still requires a control strategy to enable submicrometer patterning. In this regard, the organosilane SAMs used here on Si substrates have less desirable properties than the thiol-based SAMs on either Au or Ag as patterning inks.

There are several features which we believe lead to the improvement in the printing ability of DTS on Si over OTS. The most important of these, we believe, is that the vapor pressure of DTS is lower. By reduction of the vapor pressure, the adsorbate transport that leads to lateral line spreading is clearly inhibited.

One potential use for patterned thin films is as resists in wet chemical etching of silicon. Ideally, the μ-CP deposited SAM would function as a "negative" contrast resist, with the thin film protecting the silicon substrate in the contact regions. To accomplish this, the film must be robust enough to withstand the etching conditions. The silane SAMs described in the literature to this point do not enable any transfer of this latent image into the etched sample. We believe, for example, that OTS films are rapidly destroyed in the wet etching process. DTS, having a longer hydrocarbon chain, might prove to be more resistant to the etching solution. As shown above, DTS films printed at both room and elevated temperatures (with no postprinting treatments) do, in fact, partially protect the underlying Si substrate during etching in basic etching solutions. The structures obtained contain numerous defects, the pattern of which is reminiscent of the island motifs seen in the AFM images of the printed films (they resemble a grainlike structure). If this failure pattern does in fact reflect the grain structure of the DTS film, one expects that the thermal history of the sample should be a very sensitive control parameter. For example, heating might either coarsen the grain pattern, or, at higher temperatures, lead to the irreversible disordering of the DTS films.

It is therefore very intriguing to note that samples annealed in air prior to etching provided the best etching results. SEM images showed that this postprinting thermal treatment leads to a protection of the substrate by the film that is improved by many orders of magnitude. Defects in the patterned lines are visible, suggesting that the film is not completely stable under these conditions. Even so, the dramatic improvement seen in this simple elaboration of the molecular structure of the ink suggests that further improvements might be possible with suitable design of the adsorbate. We believe that the dramatic improvement seen between OTS and DTS suggests that self-assembled films can be engineered to give the properties needed to reduce the defect densities to acceptable levels. We will discuss this issue further in later publications.

Acknowledgment. This work was supported by the National Science Foundation (Grant CHE 9626871) and DARPA (Navy Harvard 98-15). XPS and imaging studies were carried out at the Center for Microanalysis of Materials, University of Illinois, which is supported by the Department of Energy under Contract DEFG02-91ER45439.

LA000245P

(70) The spectra shown in Figures 5 and 6 correspond closely to those reported in the literature for OTS, which, in turn, have been quantitively modeled on the basis of the optics summarized in the text. See refs: Hoffmann, H.; Mayer, U.; Krischanitz, A. *Langmuir* **1995**, *11*, 1304−1312. Allara, D. L. *Crit. Rev. Surf. Chem.* **1993**, *2*, 91−110. Parikh, A. N.; Allara, D. L. *J. Chem. Phys.* **1992**, *96*, 927−945. Hoffmann, H.; Mayer, U.; Brunner, H.; Krischanitz, A. *J. Mol. Struct.* **1995**, *349*, 305−308. Jeon, N. L.; Finnie, K.; Branshaw, K.; Nuzzo, R. G. *Langmuir* **1997**, *13*, 3382−3391. Porter, M. D.; Bright, T. B.; Allara, D. L.; Kuwana, T. *Anal. Chem.* **1986**, *58*, 2461−2465.